SCIENCE CHINA
Chemistry

• ARTICLES •

doi: 10.1007/s11426-015-5358-1

Monodispersed AuPd nanoalloy: composition control synthesis and catalytic properties in the oxidative dehydrogenative coupling of aniline

Fangyu Fu, Sen He, Sha Yang, Chen Wang, Xun Zhang, Peng Li, Hongting Sheng* & Manzhou Zhu*

Department of Chemistry and Center for Atomic Engineering of Advanced Materials, Anhui University, Hefei 230601, China

Received November 14, 2014; accepted December 15, 2014

A series of AuPd@C nanoalloy catalysts with tunable compositions were successfully prepared by a co-reduction method. The use of borane-*tert*-butylamine complex as reductant and oleylamine as both solvent and reductant was very effective for the preparation of the monodispersed nanoalloy. We evaluated the catalytic activity of these AuPd@C nanoalloys for oxidative dehydrogenative coupling of aniline, which showed better catalytic activity than equal amounts of sole Au@C or Pd@C catalyst. The Au_1Pd_3@C catalyst exhibited the best performance, indicating that the conversion and selectivity were improved along with the increase of Pd composition. However if the Pd composition was too high in the AuPd alloy, Au_1Pd_7@C achieved only 81% conversion in this reaction.

AuPd, alloy, catalyst, oxidative coupling

1 Introduction

Bimetallic nanoparticles (NPs) have received great attention for their magnetic, optical, and catalytic properties [1–8]. Compared to monometallic nanocrystals, bimetallic NPs ranging from core-shell structures to alloy have excellent physical and chemical properties because of the different geometric and electronic structures caused by the introduction of foreign metals [9–13]. The bimetallic NPs have unusual functionality due to the synergistic effects between two different metals. Notable breakthroughs have been made toward synthesizing well-defined NPs to elucidate the underlying relationship between catalytic activity and catalyst properties such as size, shape and composition [14,15].

Pt-based or Pd-based bimetallic nanostructures used as catalysts often show better selectivity, activity, and stability than NPs of the parent metals [16–19]. Of these, the AuPd bimetallic system, including core-shell, alloy, etc., has drawn wide attention in the fields of surface-enhanced Raman scattering (SERS), DAFCs electrocatalysis, organic catalysis, and so forth [20–26]. For example, Sakurai and coworkers [27] demonstrated a simple and versatile method for the preparation of bimetallic AuPd nanoclusters with controlled atomic gold distributions and stabilization by poly(vinyl-2-pyrrolidone), which are highly active and selective catalysts for the dehydrogenative aromatization of tetralin into naphthalene. In addition, Chen *et al*. [28] reported geometrically controlled nanoporous AuPd bimetallic catalysts with higher catalytic activity for direct ethanol fuel cells.

In this work, we employed a co-reduction method to synthesize a series of AuPd alloy NPs with tunable compositions by using borane-*tert*-butylamine as reductant and oleylamine (OA) as both solvent and reductant. These alloys were supported on the activated carbon, which is notable

*Corresponding authors (email: sht_anda@126.com; zmz@ahu.edu.cn)

because it showed that these AuPd@C nanoalloy catalysts are highly active as catalysts for the oxidative dehydrogenative coupling of aniline.

2 Experimental

2.1 Materials and instruments

All of the chemicals and reagents are commercially available and were used as received. Thin-plate chromatography (TLC) used commercial Merck Silica Gel 60 F254 (USA) for analytical TLC Merck Kieselgel 200-300 (USA) was used in preparative column chromatography. ^{1}H NMR spectra were acquired on a Brucker AM 400 (Switzerland) operating at 400 MHz (solvent: $CDCl_3$). ^{13}C NMR spectra were acquired on a Bruker AM 400 (Switzerland) operating at 100 MHz (solvent: $CDCl_3$). The yield and selectivity of product were performed on GC 2010 Plus from Shimadu (Japan). Transmission electron microscopy (TEM) images were obtained using a JEM 2100 microscope (Japan) and high-resolution transmission electron microscopy (HRTEM) was assessed using a JEOL-2010F instrument (Japan). Powder X-ray diffraction (XRD) patterns were collected on an MXP18AHF diffractometer (China) with Cu-Kα radiation (λ=1.54178 Å). Elemental analysis was carried out by inductively coupled plasma-atomic emission spectrometry (ICP-AES) using an Atomscan Advantage instrument made by Thormo Jarrell Ash Corporation (USA).

2.2 Preparation of AuPd NPs

$PdCl_2$ (8.7 mg, 0.049 mmol) and $HAuCl_4$ (0.098 mL, 0.049 mmol) with 1:1 molar ratio were dissolved in oleylamine (5 mL) and heated to 333 K. Next, a solution of borane-*tert*-butylamine (100 mg, 1.15 mmol) in oleylamine (1 mL) was added quickly when the solution color turned to black, after which it was heated to 363 K and kept for 30 min before being cooled down to room temperature. The crude products were washed by ethanol followed by centrifugation. A similar synthetic process was used for a different Pd/Au ratio.

2.3 Preparation of immobilized catalyst

The AuPd NPs and activated carbon with mass ratio 5:100 were dispersed in hexane (5 mL), ethanol (15 mL) as well as glacial acetic acid (1 mL) and stirred for 1 h, then filtrated with washing by deionized water and dried at 353 K to prepare the AuPd@C catalyst.

2.4 Typical procedure for the oxidative dehydrogenative coupling of aniline

A Schlenk flask was charged with aniline (0.2 mL, 2.19 mmol), KOH (0.1229 g, 2.19 mmol), catalyst (1% based on initial aniline) and 5 mL DMSO. After stirring at 333 K for 12 h under the O_2 balloon, the reaction was completed. The reaction was tracked by TLC analysis. The mixture was rotaevaporated to dryness under vacuum and purified by silica-gel column chromatography. The product was analyzed by GC.

3 Results and discussion

3.1 Synthesis and characterization of AuPd alloy NPs

A co-reduction method was employed to prepare AuPd alloy NPs. It is known that the use of amine-borane complex as reductant is very effective for the preparation of monodispersable NPs. For example, Li and coworkers [29] reported that uniform PdAg NPs could be synthesized by borane-*tert*-butylamine complex. Sun *et al*. [30] reported that monodisperse Pd NPs could be synthesized by tributylamine-borane complex. The compositions of AuPd alloy NPs were controlled by varying the molar ratios of the precursors. Therefore, thanks to the use of TBAB as an effective reductant, monodisperse NPs could be prepared under our experimental conditions. Figure 1 shows the representative TEM image of Au_1Pd_3 with a spherical shape, which is monodispersed particle of narrow size distribution (average diameter around 4.75 nm). Moreover, the broader applicability of this strategy for ultrasmall and uniform alloy was validated by the analogous preparation of AuPd alloy NPs with different compositions. By adjusting the Au-to-Pd molar ratios, a series of ultrasmall and uniform AuPd alloy NPs were achieved: these were also characterized by TEM (Figure 2). Detailed characterization of the as-obtained AuPd alloy NPs shows that they are uniform in size with an average diameter of ca. 4 nm. The HRTEM images inserted in Figures 1 and 2 exhibit the well-defined crystalline structures of the AuPd alloy NPs.

Evidence of the formation of AuPd alloy NPs is shown in the XRD patterns (Figure 3). The diffraction peaks are composed of the standard peaks between Au (JCPDS No. 65-8601) and Pd (JCPDS No. 65-6174). In other words, it is noticeable that the 2θ values of AuPd NPs lie between those of pure Au and Pd, which demonstrates the formation of single-phase AuPd alloy NPs. The peaks are noted to continuously shift from the Au standard peak to those of Pd when the content of Pd was increased. Importantly, the exact atomic ratios in the as-prepared AuPd alloy NPs were further determined by ICP-AES, which confirmed that the exact Au/Pd ratios in the as-obtained bimetallic NPs followed the trend of the designed compositions.

3.2 Characterization of immobilized AuPd@C catalyst

The sol-immobilisation method permitted the synthesis of

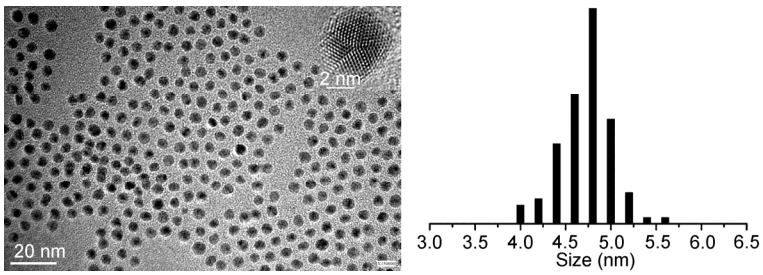

Figure 1 TEM image of the as-prepared Au_1Pd_3 nanoalloy.

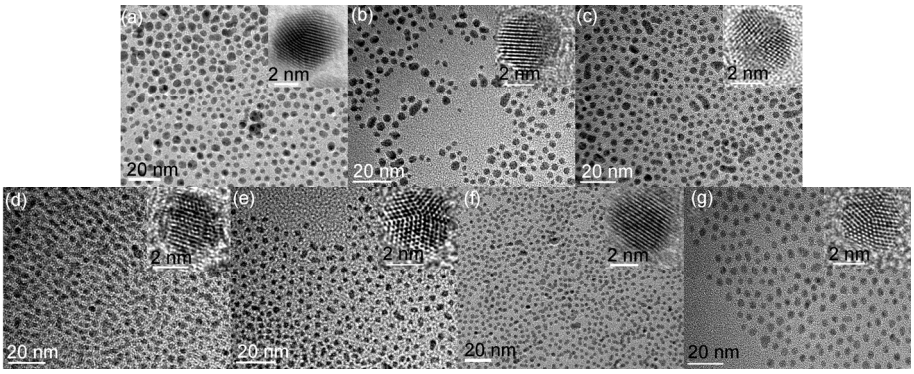

Figure 2 TEM images of the as-prepared samples. (a) Au; (b) Au_3Pd_1; (c) Au_2Pd_1; (d) Au_1Pd_1; (e) Au_1Pd_2; (f) Pd; (g) Au_1Pd_7.

NPs that could subsequently be supported on activated carbon. AuPd alloy NPs were prepared and immobilized onto carbon and dried at 353 K. The evaluation of the particle-size distributions of the colloidal metal NPs, after immobilisation on the support, is displayed in Figure 4, the typical Au_3Pd_1 and Au_1Pd_3 were examined by TEM. The particle sizes of the Au_3Pd_1 and Au_1Pd_3 were about 4 nm on the carbon supports, and the range of particle diameters was between 3 and 6 nm in diameter. It is interesting to note that the AuPd particles supported on carbon retained the same spherical shape and particle size as found in the starting AuPd alloy NPs (Figure 1). Furthermore, those are uniformly distributed on the carbon.

3.3 Catalytic tests for oxidative dehydrogenative coupling of aniline

The supported AuPd NPs were investigated for the oxidative dehydrogenative coupling of aniline to produce the azobenzene. Li *et al*. [31] reported that various monodispersed metal NPs could efficiently activate molecular oxygen under mild conditions, as illustrated by the aerobic oxidation of anilines to form either symmetric or asymmetric aromatic azo compounds. The effects of reaction temperature and O_2 were optimized by the experiment catalyzed by Au_1Pd_1@C, in terms of catalyst activity and selectivity (Table 1). The reaction temperature and O_2 affected their catalytic performance. If the reaction was conducted at room temperature and used air as the oxidant, the catalytic activity was low. However, when O_2 was used as the oxidant and reacted at 333 K, its conversion reached 55%. It is worth mentioning that the selectivity was very high when the reaction was catalyzed by 5% Au_1Pd_1@C, but low when the reaction was catalyzed by unsupported Au_1Pd_1 nanoalloy. This result indicates that the activated carbon plays a significant role in this reaction.

We chose this optimized reaction condition to study the synergistic effects between Au and Pd. As shown in Table 2, compared to the Au_1Pd_1@C catalyst, with the increase of Au composition, the conversion rose from 55% to 83% (Au_3Pd_1@C). However, the selectivity dramatically decreased to 36% (the byproduct is (*Z*)-1,2-diphenyldiazene oxide). Au@C represented high selectivity (95%), which shows that Au is an effect catalyst for this reaction [32]. Although there was a dramatic rise in conversion, from 55% to 98% (Au_1Pd_3@C), with the increase of Pd composition the selectivity remained at a high level (99%). This phenomenon indicated that in this alloy system, when Au was dominant, a small mount of Pd triggered the reduction of selectivity. In stark contrast, when the Pd was occupied the dominant status in the alloy, the Pd would be conducted to catalyzing this reaction. To our great delight, the obtained Au_1Pd_3@C catalyst exhibited the best catalytic activity. However if the Pd composition was too high in the AuPd alloy, Au_1Pd_7@C achieved only 81% conversion in this reaction. Au_1Pd_3@C was also better than the supported pure Au or Pd catalysis, which indicated that Au_1Pd_3 alloy NPs present excellent synergistic effects between two different metals.

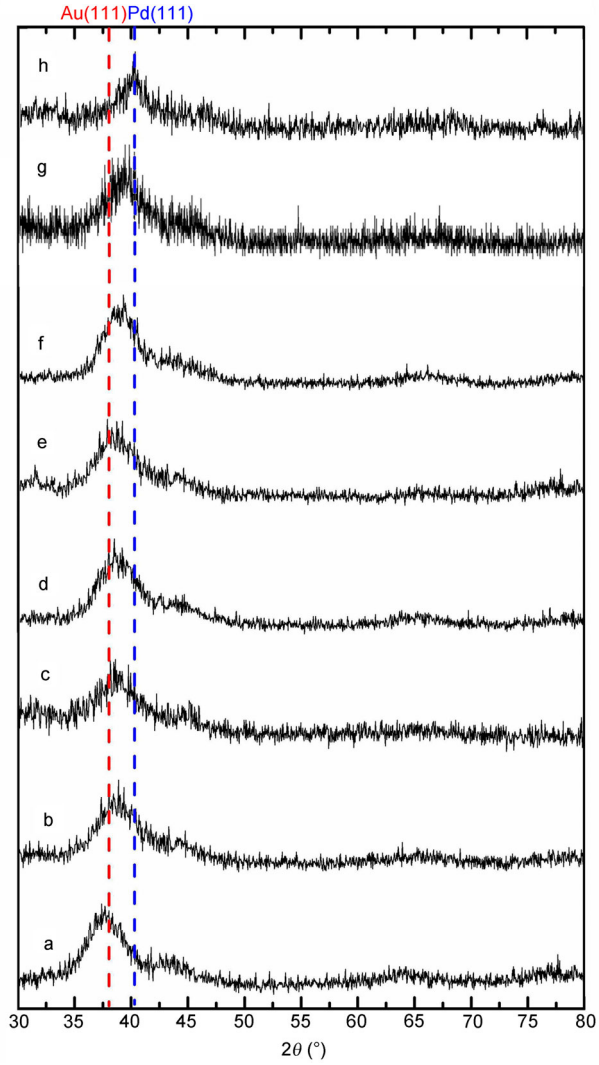

Figure 3 XRD patterns of the as-prepared samples. (a) Au; (b) Au_3Pd_1; (c) Au_2Pd_1; (d) Au_1Pd_1; (e) Au_1Pd_2; (f) Au_1Pd_3; (g) Au_1Pd_7; (h) Pd.

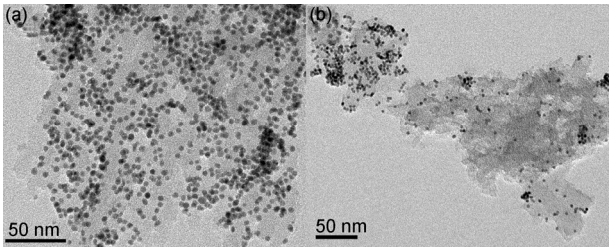

Figure 4 TEM images of 5% Au_3Pd_1@C catalyst (a) and 5% Au_1Pd_3@C catalyst (b).

3.4 Spectroscopic characterization of products

3.4.1 Azobenzene

^{1}H NMR (400 MHz, $CDCl_3$) δ (ppm): 7.93 (d, J=7.3 Hz, 4H), 7.58 (m, 6H); ^{13}C NMR (101 MHz, $CDCl_3$) δ (ppm): 152.66, 131.31, 129.16, 122.86.

Table 1 Catalytic activity of the oxidative dehydrogenative coupling of aniline with 5% Au_1Pd_1@C [a)]

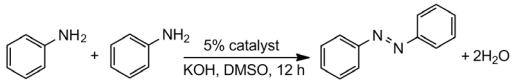

Condition	Conversion (%)	Selectivity (%)
air, r.t.	trace	99
O_2, r.t.	20	96
air, 333 K	17	98
O_2, 333 K	55	98
O_2, 333 K [b)]	18	95
O_2, 333 K [c)]	no reaction	no reaction

a) Reaction conditions: 0.2 mL aniline, catalyst loading (1% based on initial aniline), 0.1229 g KOH and 5 mL DMSO. The conversion and selectivity are performed by GC; b) catalyzed by unsupported Au_1Pd_1 nanoalloy; c) without KOH.

Table 2 Catalytic activity of oxidative dehydrogenative coupling of aniline with different catalysts [a)]

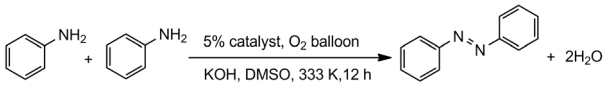

Catalyst	ICP	Conversion (%)	Selectivity (%)
Au@C	–	75	95
Au_3Pd_1@C	6.8:1	83	36
Au_2Pd_1@C	4.2:1	72	80
Au_1Pd_1@C	1.3:1	55	98
Au_1Pd_2@C	1:2.0	91	95
Au_1Pd_3@C	1:3.1	98	99
Au_1Pd_7@C	1:10.2	81	90
Pd@C	–	80	90

a) Reaction conditions: 0.2 mL aniline, catalyst loading (1% based on initial aniline), 0.1229 g KOH, and 5 mL DMSO. The conversion and selectivity were performed by GC.

3.4.2 (*Z*)-1,2-Diphenyldiazene oxide

^{1}H NMR (400 MHz, $CDCl_3$) δ (ppm): 7.38 (t, 3J=7.36 Hz, 1H, CH), 7.52 (m, 5H, CH), 8.17 (m, 2H, CH), 8.30 (m, 2H, CH); ^{13}C NMR (100 MHz, $CDCl_3$) δ (ppm): 144.04, 131.58, 129.60, 128.80, 128.70, 125.53, 122.36.

4 Conclusions

We demonstrated a co-reduction method for the synthesis of monodispersed AuPd NPs with tunable compositions. The well-defined crystalline structures and XRD patterns prove that these AuPd NPs are alloy. Significantly, thanks to the effect of palladium substitution, the as-prepared AuPd@C catalysts demonstrated superior catalytic properties for the oxidative dehydrogenative coupling of aniline to produce the azobenzene. For the as-prepared AuPd NPs, the obtained heteroatom bonds changed the electronic environment of the metal surface and the modification of its electronic structure contributed the excellent catalytic activity. This method could be extended to the synthesis of other metal-alloy catalysts in the foreseeable future.

This work was supported by the National Natural Science Foundation of China (21072001, 21372006), the Ministry of Education, the Ministry of Human Resources and Social Security, the Education Department of Anhui Province, the Anhui Province International Scientific and Technological Cooperation Project, the Natural Science Foundation of Education Department of Anhui Province (KJ2014A013), and the 211 Project of Anhui University.

1 Wang DS, Li YD. One-pot protocol for Au-base hybrid magnetic nanostructure via a noble-metal-induced reduction process. *J Am Chem Soc*, 2010, 132: 6280–6281
2 Lu AH, Salabas EL, Schueth F. Magnetic nanoparticles: synthesis, protection, functionalization, and application. *Angew Chem Int Ed*, 2007, 46: 1222–1244
3 Xiang J, Li P, Chong HB, Feng L, Fu FY, Wang Z, Zhang SL, Zhu MZ. Bimetallic Pd-Ni core-shell nanoparticles as effective catalysts for the Suzuki reaction. *Nano Res*, 2014, 7: 1337–1343
4 Klimov VI, Ivanov SA, Nanda J, Achermann M, Bezel I, McGuire JA, Piryatinski A. Single-exciton optical gain in semiconductor nanocrystals. *Nature*, 2007, 447: 441–446
5 Yang Y, Chen O, Angerhofer A, Cao YC. Radial-position-controlled doping in CdS/ZnS core/shell nanocrystals. *J Am Chem Soc*, 2006, 128: 12428–12429
6 Raimondi F, Scherer GG, Koetz R, Wokaun A. Nanoparticles in energy technology: examples from electrochemistry and catalysis. *Angew Chem Int Ed*, 2005, 44: 2190–2209
7 Roucoux A, Schulz J, Patin H. Reduced transition metal colloids: a novel family of reusable catalysts? *Chem Rev*, 2002, 102: 3757–3778
8 Niu ZQ, Wang DS, Yu R, Peng Q, Li YD. Highly branched Pt-Ni nanocrystals enclosed by stepped surface for methanol oxidation. *Chem Sci*, 2012, 3: 1925–1929
9 Saleem F, Zhang ZC, Xu B, Xu XB, He PL, Wang X. Ultrathin Pt-Cu nanosheets and nanocones. *J Am Chem Soc*, 2013, 135: 18304–18307
10 Wang SX, Meng XM, Das A, Li T, Song YB, Cao TT, Zhu XY, Zhu MZ, Jin RC. A 200-fold quantum yield boost in the photoluminescence of silver-doped Ag_xAu_{25-x} nanoclusters: the 13th silver atom matters. *Angew Chem Int Ed*, 2014, 53: 2376–2380
11 Snyder J, McCue I, Livi K, Erlebacher J. Structure/processing/properties relationships in nanoporous nanoparticles as applied to catalysis of the cathodic oxygen reduction reaction. *J Am Chem Soc*, 2012, 134: 8633–8645
12 Chen W, Yu R, Li LL, Wang AN, Peng Q, Li YD. A seed-based diffusion route to monodisperse intermetallic CuAu nanocrystals. *Angew Chem Int Ed*, 2010, 49: 2917–2921
13 Zhu C, Peng HC, Zeng J, Liu JY, Gu ZZ, Xia YN. Facile synthesis of gold wavy nanowires and investigation of their growth mechanism. *J Am Chem Soc*, 2012, 134: 20234–20237
14 Hansgen DA, Vlachos DG, Chen JG. Using first principles to predict bimetallic catalysts for the ammonia decomposition reaction. *Nat Chem*, 2010, 2: 484–489
15 Hong JW, Kim D, Lee YW, Kim M, Kang SW, Han SW. Atomic-distribution-dependent electrocatalytic activity of Au-Pd bimetallic nanocrystals. *Angew Chem Int Ed*, 2011, 50: 8876–8880
16 Yu WT, D Porosoff MG, Chen JG. Review of Pt-based bimetallic catalysis: from model surfaces to supported catalysts. *Chem Rev*, 2012, 112: 5780–5817
17 Xi PX, Cao Y, Yang FC, Ma C, Chen FJ, Yu S, Wang S, Zeng ZZ, Zhang X. Facile synthesis of Pd-based bimetallic nanocrystals and their application as catalysts for methanol oxidation reaction. *Nanoscale*, 2013, 5: 6124–6130
18 Kang SW, Lee YW, Park Y, Choi BS, Hong JW, Park KH, Han SW. One-pot synthesis of trimetallic Au@PdPt core-shell nanoparticles with high catalytic performance. *ACS Nano*, 2013, 7: 7945–7955
19 Xia YN, Xiong YJ, Lim B, Skrabalak SE. Shape-controlled synthesis of metal nanocrystals: simple chemistry meets complex physics. *Angew Chem Int Ed*, 2008, 48: 60–103
20 Wang AN, Peng Q, and Li YD. Rod-shaped Au-Pd core-shell nanostructures. *Chem Mater*, 2011, 23: 3217–3222
21 Sarina S, Zhu HY, Jaatinen E, Xiao Q, Liu HW, Jia JF, Chen C, Zhao J. Enhancing catalytic performance of palladium in gold and palladium alloy nanoparticles for organic synthesis reactions through visible light irradiation at ambient temperatures. *J Am Chem Soc*, 2013, 135: 5793–5801
22 Liu, HY, Yang Q. Facile fabrication of nanoporous Au-Pd bimetallic foams with high catalytic activity for 2-nitrophenol reduction and SERS property. *J Mater Chem*, 2011, 21: 11961–11967
23 Pritchard J, Piccinini M, Tiruvalam R, He Q, Dimitratos N, Lopez-Sanchez JA, Morgan DJ, Carley AF, Edwards JK, Kielyb CJ, Hutchings GJ. Effect of heat treatment on Au-Pd catalysts synthesized by sol immobilisation for the direct synthesis of hydrogen peroxide and benzyl alcohol oxidation. *Catal Sci Technol*, 2013, 3: 308–317
24 Zhang L, Zhang JW, Kuang Q, Xie SF, Jiang ZY, Xie ZX, Zheng LS. Cu^{2+}-assisted synthesis of hexoctahedral Au-Pd alloy nanocrystals with high-index facets. *J Am Chem Soc*, 2011, 133: 17114–17117
25 Wang F, Li CH, Sun LD, Wu HS, Ming T, Wang JF, Yu JC, Yan CH. Heteroepitaxial growth of high-index-faceted palladium nanoshells and their catalytic performance. *J Am Chem Soc*, 2011, 133: 1106–1111
26 Hong JW, Lee YW, Kim M, Kang SW, Han SW. One-pot synthesis and electrocatalytic activity of octapodal Au-Pd nanoparticles. *Chem Commun*, 2011, 47: 2553–2555
27 Murugadoss A, Okumura K, Sakurai H. Bimetallic AuPd nanocluster catalysts with controlled atomic gold distribution for oxidative dehydrogenation of tetralin. *J Phys Chem C*, 2012, 116, 26776–26783
28 Chen LY, Chen N, Hou Y, Wang ZC, Li SH, Fujita T, Jiang JH, Hirata A, Chen MW. Geometrically controlled nanoporous PdAu bimetallic catalysts with tunable Pd/Au ratio for direct ethanol fuel cells. *ACS Catal*, 2013, 3: 1220–1230
29 Li LS, Niu ZQ, Cai SF, Zhi Y, Li H, Rong HP, Liu LC, Liu L, He W, Li YD. A PdAg bimetallic nanocatalyst for selective reductive amination of nitroarenes. *Chem Commun*, 2013, 49: 6843–6845
30 Mazumder V, Sun SH. Oleylamine-mediated synthesis of Pd nanoparticles for catalytic formic acid oxidation. *J Am Chem Soc*, 2009, 131: 4588–4589
31 Cai SF, Rong HP, Yu XF, Liu XW, Wang DS, He W, Li YD. Room temperature activation of oxygen by monodispersed metal nanoparticles: oxidative dehydrogenative coupling of anilines for azobenzene syntheses. *ACS Catal*, 2013, 3: 478–486
32 Grirrane A, Corma A, Garcia H. Gold-catalyzed synthesis of aromatic azo compounds from anilines and nitroaromatics. *Science*, 2008, 322: 1661–1664